JOURNAL OF GEOPHYSICAL RESEARCH, VOL. 115, D00K09, doi:10.1029/2009JD012757, 2010

Asian dust over northern China and its impact on the downstream aerosol chemistry in 2004

Yele Sun,[1,2,3] Guoshun Zhuang,[1,3] Kan Huang,[1] Juan Li,[1] Qiongzhen Wang,[1] Ying Wang,[1,3] Yanfen Lin,[1] Joshua S. Fu,[4] Wenjie Zhang,[3] Aohan Tang,[3] and Xiujuan Zhao[3]

Received 29 June 2009; revised 7 November 2009; accepted 13 January 2010; published 3 June 2010.

[1] TSP and $PM_{2.5}$ aerosol particles were synchronously sampled at six sites along the transport pathway of dust storms from desert regions to coastal areas in the spring of 2004 to investigate the regional characteristics of Asian dust and its impact on aerosol chemistry over northern China. Factor analysis of daily PM_{10} concentrations in 17 cities showed that northern China can be basically divided into five regions: (1) Northern Dust Region, (2) Northeastern Dust Region, (3) Western Dust Region, (4) Inland Passing Region, and (5) Coastal Region. Northern Dust Region was characterized by a high content of Ca. Northeastern Dust Region was a relatively clean area with a low concentration of pollutants and secondary ions in comparison to other regions. Inland Passing Region and Coastal Region showed high concentrations of anthropogenic pollutants. The impact of Asian dust on aerosol chemistry decreased in the order Yulin/Duolun > Beijing > Qingdao/Shanghai as transport distance increased. The ratio of Ca/Al, which showed significant differences in different regions over northern China, is suggested to be a tracer to identify the sources of dust storms. Asian dust either mixes pollutants on the pathway and carries them to the downwind regions or dilutes the pollutants over northern China, which affects the aerosol composition more in coarse particles in those areas near source regions and more in fine particles in downwind areas. The ratio of NO_3^-/SO_4^{2-} during dust storms was significantly reduced and the lowest generally appeared after the peak of dust. Our results showed that Asian dust plays a critical role in buffering the acidity of aerosols over northern China by a potential increase of ~1 unit pH for the aerosol particles in spring.

Citation: Sun, Y., et al. (2010), Asian dust over northern China and its impact on the downstream aerosol chemistry in 2004, *J. Geophys. Res.*, *115*, D00K09, doi:10.1029/2009JD012757.

1. Introduction

[2] Asian dust storms, picked up by strong winds from central Asia and Gobi deserts, have aggrieved northern China for centuries [*Sun et al.*, 2004b; *Zhuang et al.*, 2001], and plague Korea, Japan, the North Pacific Ocean and as far as the American continent through long-range transport as well [*Duce et al.*, 1980; *Husar et al.*, 2001; *In and Park*, 2002; *Uematsu et al.*, 2002]. Asian dust from arid and semiarid areas of Mongolia and northern China forms dust clouds and sweeps over most of northern China in a few days. As a dust cloud travels downstream, it could mix with industrial pollutants, toxic metals, soot, and gas pollutants on the pathway [*Huebert et al.*, 2003], and further interact with sea salt over the ocean [*D. Zhang et al.*, 2003]. The mixing and interactions of dust with pollution aerosol on the pathway have significant effects on the size distribution and chemical composition of aerosol downstream [*Sun et al.*, 2005; *Wang et al.*, 2007] and hence the direct/indirect radiative forcing on climate. For example, anthropogenic SO_2 could be incorporated into the advecting dust plumes via heterogeneous SO_2 oxidation over the Yellow Sea [*Meskhidze et al.*, 2003] and change the distribution of Fe (III)/Fe(II), which has a potential impact on the ocean productivity via the long-range transport [*Duce et al.*, 1980; *Jickells et al.*, 2005; *Zhuang et al.*, 1992]. Asian dust and the unique characteristic of pollution in Chinese cities rightly provide a special platform to study the mixing between dust and pollution aerosol.

[3] Dust storms (DS) in northern China show typically regional characteristics. Using a rotated empirical orthogonal function and the annual days of DS from 1954 to 1998,

[1]Center for Atmospheric Chemistry Study, Department of Environmental Science and Engineering, Fudan University, Shanghai, China.
[2]Now at Department of Environmental Toxicology, University of California, Davis, California, USA.
[3]Center for Atmospheric Environmental Study, Department of Chemistry, Beijing Normal University, Beijing, China.
[4]Department of Civil and Environmental Engineering, University of Tennessee, Knoxville, Tennessee, USA.

0148-0227/10/2009JD012757

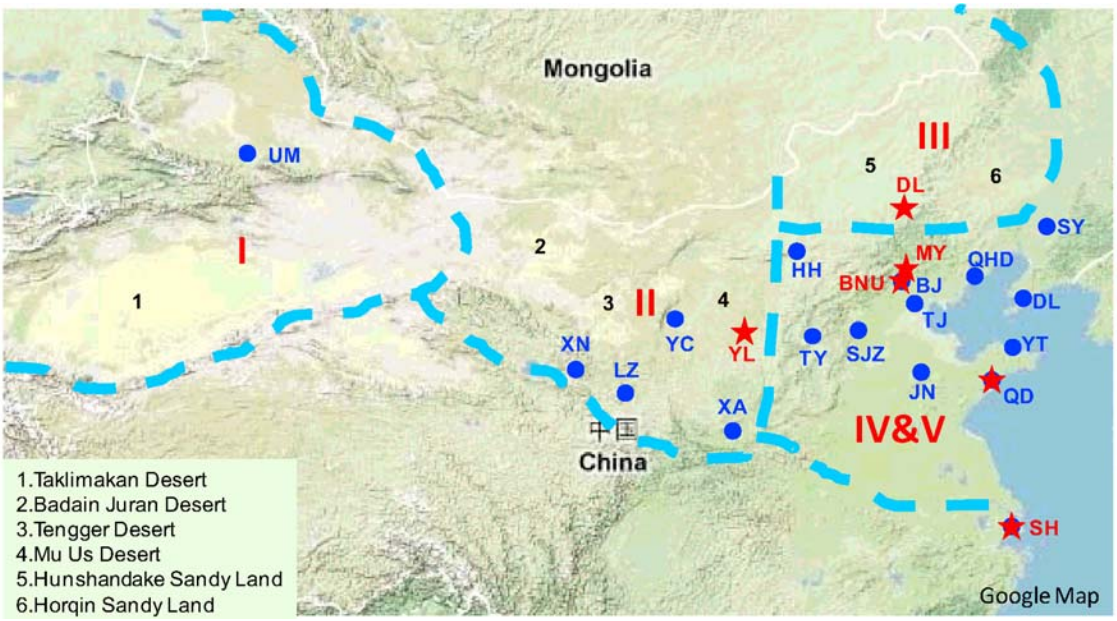

Figure 1. Potential regional division of the cities over northern China in the spring of 2004 (I, Western Dust Region; II, Northern Dust Region; III, Northeastern Dust Region; and IV and V, Inland Passing Region and Coastal Region). The sampling sites are marked as red stars. The cities where the PM_{10} data were used for factor analysis are marked as blue dots (SY, Shenyang; DL, Dalian; YT, Yantai; QD, Qingdao; QHD, Qinhuangdao; BJ, Beijing; TJ, Tianjin; JN, Jinan; SJZ, Shijiazhuang; TY, Taiyuan; HH, Hohhot; XA, Xi'an; YC, Yinchuan; LZ, Lanzhou; XN, Xining; and UM, Urumchi).

Qian et al. [2004] observed five different regions associated with DS. They were Xinjiang region, the eastern part of inner Mongolia, Tsaidam Basin, Tibetan Plateau, and Gobi Desert near Yellow River. *S. Wang et al.* [2005] investigated the regional characteristics of DS, blowing dust, and floating dust in China using the data collected from 701 meteorological observation stations from 1954 to 2004. The three types of dust events showed significantly different spatial distribution. They found that DS occurred most frequently in the arid and semiarid areas in northern China and blowing dust and floating dust occurred in both these areas and their neighboring areas. While the regional characteristics of DS are well understood, the distribution of aerosol components in different regions as well as the impact from Asian dust is rather limited.

[4] The Aerosol Characterization Experiments (ACE-Asia) organized by the International Global Atmospheric Chemistry (IGAC) Program increased our knowledge of the mixing of dust with pollution aerosol. The dust, transported halfway around the globe, is not just dust: it is the mixture of dust with pollution. Air pollution changes dust aerosols in many ways, adding black carbon, toxic materials, and acidic gases to the mineral particles [*Huebert et al.*, 2003]. During the ACE-Asia campaign, *X. Y. Zhang et al.* [2003] found that the contents of Ca and Fe were up to 12% and 6%, respectively, in western high dust source regions, higher than those in other source regions, whereas the content of Al was ~7% among all of major source regions. As such, *Arimoto et al.* [2004] observed significantly different composition of aerosols between Zhenbeitai in China and Gosan in South Korea. This difference was likely from the different extent of mixing and interaction between dust and pollution during the long-range transport. The synchronous monitoring aerosol at desert region and coastal Yellow Sea also suggested the strong spatial variation of trace elements and confirmed the impact of mineral aerosol from northwest desert regions on the distribution of trace elements over Yellow Sea in spring [*Liu et al.*, 2002]. However, these studies were mostly restricted to either a single sampling site or limited aerosol components.

[5] In a previous study, *Wang et al.* [2007] reported the difference of three major components of aerosol, i.e., crustal, secondary, and carbonaceous material between dust and nondust storm (NDS) days. The source contributions from the upstream and the pathways of Asian dust were calculated to account for 49%, 82%, and 28% of particulate matter (PM), crust, and secondary aerosol, respectively, and the contributions of crust and secondary aerosol decreased as the DS progressed eastward. In this study, we propose the regional division of northern China for aerosol characterization, comprehensively investigate the spatial distribution of aerosol components including elements and ions, and evaluate the impact of Asian dust on aerosol composition and acidity downstream.

2. Experimental Methods

2.1. Sampling

[6] Aerosol particles of TSP and $PM_{2.5}$ were synchronously sampled at Yulin (YL) in Shanxi province, Duolun (DL) in Inner Mongolia, Beijing, including an urban site at Beijing Normal University (BNU) and a suburban site at Miyun (MY), Qingdao (QD), and Shanghai (SH) (Figure 1) in the spring of 2004. The detailed descriptions of these

Table 1. Varimax Rotated Factor Loading Matrix for PM_{10} in 17 Cities Over Northern China[a]

Cities	Factor 1	Factor 2	Factor 3	Factor 4
Lanzhou	0.20	0.02	**0.78**	−0.27
Xi'an	−0.03	0.15	**0.73**	0.14
Xining	0.21	0.11	**0.81**	−0.24
Yinchuan	0.30	−0.07	**0.79**	0.19
Beijing	**0.89**	−0.04	0.17	0.01
Hohhot	**0.72**	0.11	0.26	−0.07
Shijiazhuang	**0.72**	0.21	0.37	0.12
Taiyuan	**0.69**	0.26	0.02	0.02
Tianjin	**0.87**	0.18	0.12	−0.08
Qinhuangdao	**0.82**	0.10	0.01	0.07
Jinan	0.40	0.57	0.20	0.24
Qingdao	−0.07	**0.87**	0.16	−0.14
Yantai	0.25	**0.62**	−0.24	−0.27
Dalian	0.44	**0.66**	0.05	0.08
Shanghai	−0.05	**0.76**	0.06	0.07
Shenyang	0.31	**0.68**	0.08	0.13
Urumchi	−0.04	−0.04	0.08	**−0.85**
Expl. Var	4.46	3.16	2.82	1.13
Prp. Totl	0.26	0.19	0.17	0.07

[a]Factor loadings larger than 0.60 are marked in bold. Number is samples in the statistics: n = 61. Expl. Var, explained variance; Prp. Totl, proportion of total variance.

sampling sites were given by *Wang et al.* [2007] and *Sun et al.* [2006]. All the aerosol samples were collected on Whatman® 41 filters (Whatman Inc., Maidstone, U. K.) using medium-volume samplers manufactured by Beijing Geological Instrument-Dickel Co., Ltd. (model: TSP/PM_{10}/$PM_{2.5}$–2; flow rate: 77.59 L min^{-1}). The filters before and after sampling were weighed using an analytical balance (Sartorius 2004MP, with a reading precision of 10 μg) after keeping them in constant temperature (20 ± 1°C) and humidity (40 ± 1%) for 48 h.

2.2. Chemical Analysis

2.2.1. Element Analysis

[7] The sample filters were digested at 170°C for 4 h in high-pressure Teflon digestion vessel with 3 mL of concentrated HNO_3, 1 mL of concentrated $HClO_4$, and 1 mL of concentrated HF. After cooling, the solutions were dried and then diluted to 10 mL with distilled deionized water. In total, 23 elements (Al, Fe, Mn, Mg, Ti, Sc, Na, Eu, Ce, Sr, Ca, Co, Cr, Ni, Cu, Pb, Zn, Cd, V, S, As, Se, and Sb) were measured by inductively coupled plasma atomic emission spectroscopy (ICP-AES, Model: ULTIMA, JOBIN-YVON Company, France). The detailed analytical procedures were given elsewhere [*Zhuang et al.*, 2001].

2.2.2. Ion Analysis

[8] Eleven inorganic ions (SO_4^{2-}, NO_3^-, F^-, Cl^-, NO_2^-, PO_4^{3-}, NH_4^+, Na^+, K^+, Ca^{2+}, and Mg^{2+}) and four organic acids (acetic, formic, oxalic, and methylsulfonic acid (MSA)) were analyzed by ion chromatography (IC, Dionex 600) that consists of a separation column (Dionex Ionpac AS11 for anion and CS12A for cation), a guard column (Dionex Ionpac AG 11 for anion and AG12A for cation), a self-regenerating suppressed conductivity detector (Dionex Ionpac ED50), and a gradient pump (Dionex Ionpac GP50). The details were given elsewhere [*Yuan et al.*, 2003].

2.2.3. Air Mass Trajectory Analysis

[9] Back trajectories reaching the five cities in this study were calculated using the HY-SPLIT 4.8 (Hybrid Single Particle Lagrangian Integrated Trajectories) of National Oceanic and Atmospheric Administration (NOAA) (http://www.arl.noaa.gov/ready/hysplit4.html). The back trajectory analysis was performed with meteorological input from Air Resources Laboratory FNL data archive. More details on HYSPLIT model were given by R. R. Draxler and G. D. Rolph (HYSPLIT (HYbrid Single-Particle Lagrangian Integrated Trajectory) Model, 2003, http://www.arl.noaa.gov/ready/hysplit4.html).

2.2.4. PM_{10} Data

[10] Air pollution index (API) data in 17 cities over northern China (Figure 1) during March–April in 2004 were obtained from the State Environmental Protection Administration of China (http://www.zhb.gov.cn/quality/air.php3). Other cities such as Changchun and Haerbin were excluded in the following analysis because they are located in the far north of China and less relevant to the scope of this paper. API was converted to PM_{10} concentration according to the following formula:

$$C = C_{\text{low}} + \left[(I - I_{\text{low}})/(I_{\text{high}} - I_{\text{low}})\right] \times (C_{\text{high}} - C_{\text{low}}),$$

where C is the concentration of PM_{10} and I is the API value of PM_{10}. I_{high} and I_{low}, the two values most approaching to value I in the API grading limited value table, stand for the value larger and lower than I, respectively; C_{high} and C_{low} represent the PM_{10} concentration corresponding to I_{high} and I_{low}, respectively.

3. Results and Discussion

3.1. Regional Division of the Areas Over Northern China

[11] Dust storm leads to heavy particulate pollution over northern China. Inhalable particles (PM_{10}) are, consequently, the primary pollutants in most of cities over northern China in spring. Factor analysis (STATISTICA, 2001) of the PM_{10} data from 17 cities (Figure 1 and Table 1) suggested that the PM over northern China showed typically regional characteristics. The first factor showed high loadings for the cities of Beijing, Tianjin, Taiyuan, Shijiazhuang, Hohhot, and Qinhuangdao, most of which are located on the transport pathway of DS to downstream regions. This region was named Inland Passing Region (region IV in Figure 1). The second factor was strongly associated with Qingdao, Yantai, Dalian, Shanghai, and Shenyang. These cities are located in the coastal areas, which were named Coastal Region (region V in Figure 1). Most of the cities in the third factor, such as Lanzhou, Xinning, Yinchuan, and Xi'An, are located in central northern China and close to Tengger Desert, Badain Juran Desert, and Mu Us Desert. This region was thus named Northern Dust Region (region II in Figure 1). Urumchi showed a high loading in the fourth factor, representing Western Dust Region (region I in Figure 1), where Takalimakan Desert and Gurbantunggut Desert are located. Another region named Northeastern Dust Region (region III in Figure 1) is located near Hunshandake Sandy Land and Horqin Sandy Land, where the daily reports of primary pollutants have not been set up yet. The potential five regions shown in Figure 1 are closely associated with the distribution of population and economic growth. Region I has the least population under 10 million and the region IV

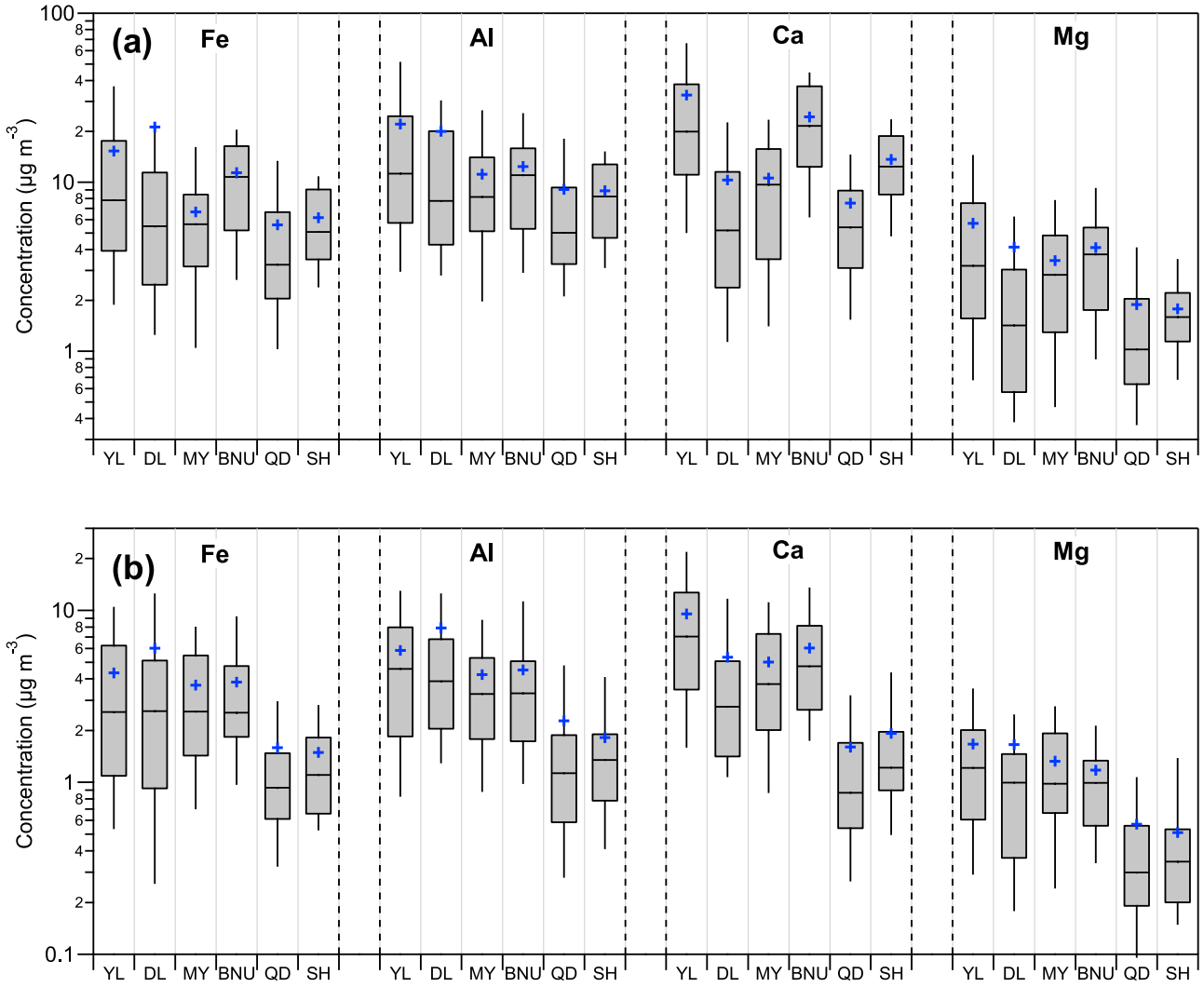

Figure 2. Spatial variations of Fe, Al, Ca, and Mg in (a) TSP and (b) $PM_{2.5}$ in the spring of 2004. Crosses represent the average mass concentration; horizontal lines represent the median; bottom and top of the boxes represent the 25 and 75% limits, respectively; and bottom and top whiskers represent the 5 and 95% limits, respectively.

and V has the most population with most of the provinces more than 40 million. The population of region II is between ~10 and 20 million and region III is between ~10 and 30 million (http://www.chinatoday.com/data/china.population.htm).

[12] The six sampling sites in this study are located in regions II, III, IV, and V. The aerosol particles at YL and DL, located in regions II and III, respectively, were observed to be dominated by crustal elements with less anthropogenic contribution [*Arimoto et al.*, 2004; *Cheng et al.*, 2005]. YL and DL are thus used as representatives of regions II and III, respectively. Regions IV and V, as described above with most of the polluted cities located over northern China, may have large contributions from local or transport anthropogenic pollution. While the suburban and urban areas could show significant different aerosol composition due to the different sources [*Sun et al.*, 2004a; *Y. Wang et al.*, 2005b], BJ and QD are selected as the representatives

Table 2. Meteorological Conditions During DS1, DS2, and NDS in the Spring of 2004

	Temperature (°C)			Relative Humidity (%)			Wind Speed (m/s)			Precipitation (mm)		
Sites	DS1	DS2	NDS	DS1	DS2	NDS	DS1	DS2	NDS	DS1	DS2	NDS
Yulin	8.4	5.6	10.1	18	11	23	3.5	5.0	2.6	0	0	3
Duolun	7.5	6.9	2.8	30	20	30	5.0	6.8	4.1	0	0	8
Beijing	9.1	16.1	13.4	41	18	30	2.0	3.8	3.0	0	0	23
Qingdao	9.4	9.7	9.8	42	29	66	5.8	4.3	4.2	0	0	399
Shanghai	17.2	13.4	13.6	48	63	68	5.0	3.8	3.6	0	0	910

Table 3. Ratios of Fe/Al, Mg/Al, and Ca/Al in TSP and $PM_{2.5}$ at Six Sampling Sites

Sites	TSP			$PM_{2.5}$			References
	Fe/Al	Mg/Al	Ca/Al	Fe/Al	Mg/Al	Ca/Al	
YL	0.65	0.27	1.64	0.70	0.30	1.71	this study
DL	0.62	0.18	0.61	0.60	0.21	0.79	this study
MY	0.63	0.32	1.01	0.85	0.33	1.17	this study
BNU	1.03	0.35	2.27	1.00	0.29	1.55	this study
QD	0.62	0.21	0.95	0.79	0.27	0.83	this study
SH	0.71	0.21	1.60	0.98	0.31	1.09	this study
Crust	0.62	0.26	0.45				*Mason and Moore* [1982]
YL	0.48	0.29	1.48				*Zhang et al.* [1996]
Dingbian[a]	0.93	0.22	1.97				*Zhang et al.* [1996]
Beijing[b]	0.58	0.27	1.34	1.22	0.28	1.41	this study
Sanggen Dalai[c]	0.85	0.26	0.64				*Cheng et al.* [2005]
Taklimakan Desert	0.69	0.55	1.65	0.82	0.62	1.70	this study
Aksu[d]	1.04	0.50	2.04				*Zhang et al.* [2003]

[a]Near Mu Us Desert.
[b]The average of 2001–2002 in Beijing.
[c]Dusty days near Hunshan Daka Sandland.
[d]Northern margin of Taklimakan Desert.

of regions IV and V, respectively, with a focus on the impact of Asian dust on the cities and the mixing of Asian dust with city anthropogenic pollution. The aerosol composition previously observed at BNU [*Sun et al.*, 2004a] is similar to those observed at other urban sites in Beijing [*He et al.*, 2001], indicating that BNU is a typical urban site with significant source contribution from traffic and coal combustion [*Dan et al.*, 2004; *Song et al.*, 2006; *Sun et al.*, 2004a]. QD, located in region V, was also used to investigate the impact of DS on aerosol composition and the mixing of dust particles with anthropogenic pollution [*Z. G. Guo et al.*, 2004; *D. Zhang et al.*, 2003]. SH was not included in the final regional division because it is beyond the scope of northern China. However, SH was involved in the discussion of the impact of Asian dust on downstream regions for additional support. The impact of Asian dust on the aerosol composition in SH was also observed in previous studies [*Wang et al.*, 2006; *Ye et al.*, 2003].

3.2. Regional Characteristics of Spring Aerosols Over Northern China

[13] The aerosols in northern China are mainly composed of mineral matter, organic material, and secondary sulfate and nitrate [*He et al.*, 2001; *Sun et al.*, 2004a; *X. Y. Zhang et al.*, 2003]. The aerosol composition shows significant regionality due to the significant differences in economic development, energy consumption, geographical location, and meteorological conditions in different regions. Since the average aerosol composition in spring over northern China would be significantly biased by the dominant loadings of DS, median aerosol composition is then used for the regional characterization. For the convenience of discussion, the aerosol components including elements and ions are divided into six groups based on their sources observed in previous studies [*Sun et al.*, 2005; *Y. Wang et al.*, 2005a, 2007]: (1) mineral elements, including Ca, Al, Fe, Na, Mg, and Ti; (2) pollution elements, including As, Zn, Pb, and Cu; (3) other elements, including Mn, V, Ni, Sr, and Cr; (4) mineral ions, including Na^+, Ca^{2+}, and Mg^{2+}; (5) secondary ions, including NH_4^+, NO_3^-, and SO_4^{2-}; and (6) other ions, including K^+, F^-, and Cl^-.

3.2.1. Variation of Mineral Elements in Different Regions

[14] Figure 2 presents the spatial variations of major mineral elements, Fe, Al, Ca, and Mg in TSP and $PM_{2.5}$. The results of one-way ANOVA test ($p < 0.05$) indicated that Fe and Al did not show, but Ca did show, significantly different spatial variations among all sites. BNU showed the highest median concentrations of Fe, Al, and Mg in TSP, followed by YL and QD. The major source of these elements is dust including road dust, soil dust, construction dust, and transported dust. The high concentration of mineral elements at BNU was associated with road dust resuspended by winds and motor vehicles [*He et al.*, 2001; *Sun et al.*, 2004a] and transported dust [*Han et al.*, 2007]. In comparison to BNU, QD in region V and SH showed much lower concentration of mineral elements which was likely due to the higher relative humidity and more precipitation (Table 2) at these two sites as well as less transported dust from northern China. The high concentrations of mineral elements at YL were associated with the frequent dust from deserts nearby [*X. Y. Zhang et al.*, 2003]. While DL is located in the dust source regions, it did not show high median concentrations of mineral elements, but the average concentrations were close to those at YL and BNU, indicating that DL was sporadically affected by DS and it was clean for most of NDS days. Comparatively, the spatial distributions of mineral elements in $PM_{2.5}$ were relatively universalistic. Fe, Al, and Mg showed relatively even distributions at four sites, YL, DL, BNU, and MY, and much higher than those at other two sites, QD and SH.

[15] The case of Ca was much different from Fe, Al, and Mg. Ca showed strong regionality in both TSP and $PM_{2.5}$. In TSP, the median concentration of Ca was in the order BNU > YL > SH > MY > QD > DL. The mass percentage of Ca at YL was 8.1%, which is close to the values of 7% in the northern high dust source areas and 8% in loess area [*X. Y. Zhang et al.*, 2003], while it was only 3.7% at DL, much lower than those in other regions. In addition, the mass percentage of Ca was much higher than the soil background value (1%–2%) in northeastern China [*Zheng et al.*, 1994]. These results further confirmed that region II is characterized by high content of Ca, while region III is

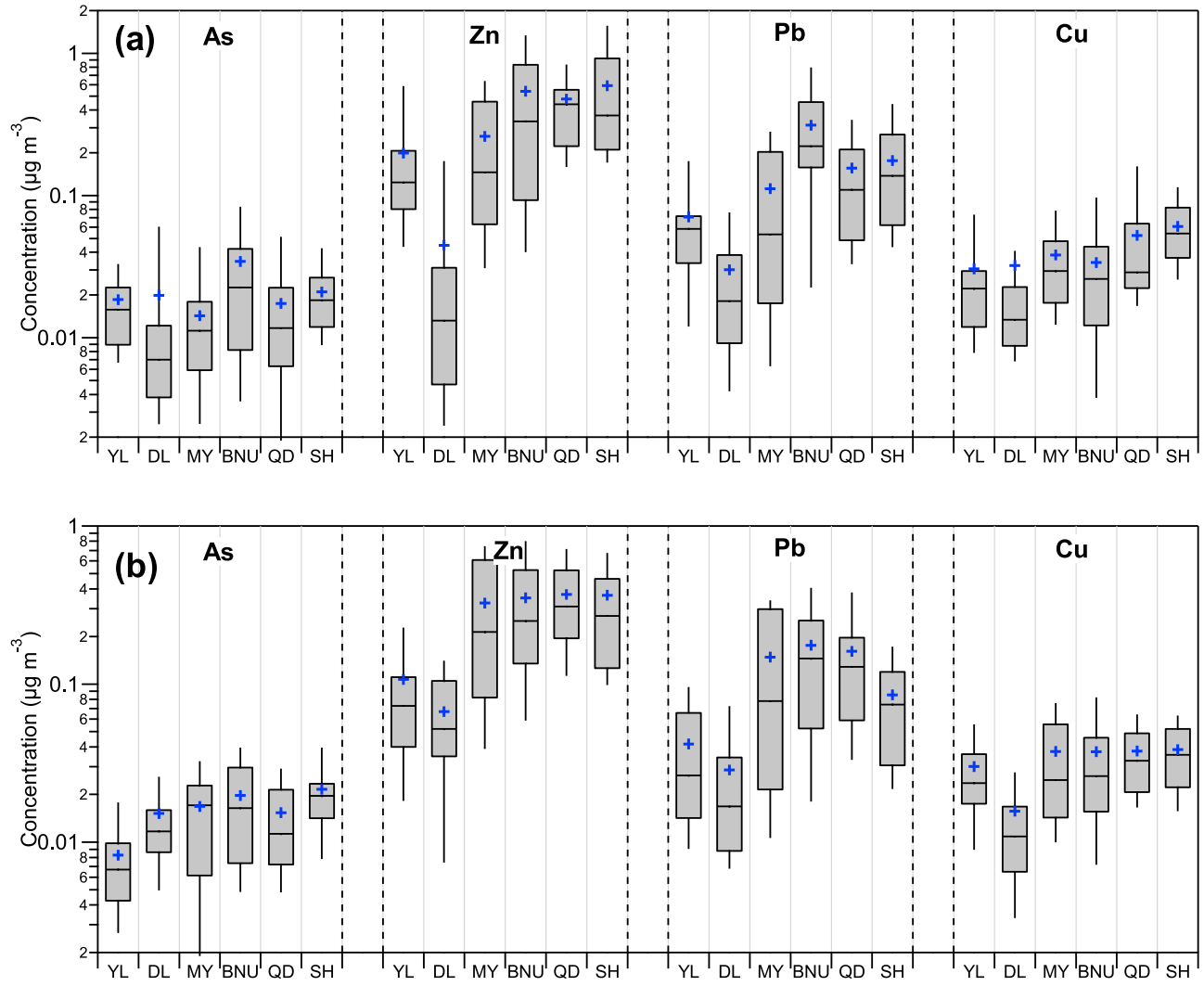

Figure 3. Spatial variations of As, Zn, Pb, and Cu in (a) TSP and (b) $PM_{2.5}$ in the spring of 2004. Crosses represent the average mass concentration; horizontal lines represent the median; bottom and top of the boxes represent the 25 and 75% limits, respectively; and bottom and top whiskers represent the 5 and 95% limits, respectively.

characterized by low concentration of Ca [*Sun et al.*, 2005; *X. Y. Zhang et al.*, 1996, 2003]. The high concentration of Ca in BJ and SH was partially due to local construction and/or road dust. The spatial distribution of Ca in $PM_{2.5}$ was slightly different from those in TSP. While YL still showed the highest Ca, the urban sites BNU, QD, and SH showed lower concentration of Ca if DL was used for a reference. These results further supported the contribution of local dust to Ca at urban sites given that Ca from dust is more attributed to coarse particles.

[16] Table 3 shows the elemental ratios of Fe/Al, Mg/Al, and Ca/Al in different regions of China. The ratios of Fe/Al at YL, DL, MY, and QD were lower than those in BJ and SH, but all were close to the 0.62 of the mean crust abundance [*Mason and Moore*, 1982] and the 0.65 of Northern Dust Region in China [*X. Y. Zhang et al.*, 2003]. The high values of Fe/Al in BJ and SH were likely due to the emission from steel industry in the two cities, such as Capital Steel Group in Beijing and Baoshan Steel Group Corporation in Shanghai, the large sources of Fe in the aerosol. The distribution of Ca/Al is similar to that of Ca. The ratio of Ca/Al was in the order BNU > YL > SH > MY > QD > DL in TSP and YL > BNU > SH > MY > QD > DL in $PM_{2.5}$. Ca/Al ratios of 1.64 in TSP and 1.71 in $PM_{2.5}$ at YL in this study were consistent with those (1.48 at YL and 1.97 at Dingbian near Mu Us Desert) reported previously by *Zhang et al.* [1996], and the ratios of Ca/Al of 0.61 in TSP and 0.79 in $PM_{2.5}$ at DL were similar to 0.64 in TSP collected during dusty days at Sanggen Dalai near Hunshandake Sandy Land [*Cheng et al.*, 2005]. These results confirmed the characteristics of high content of Ca in Northern Dust Region and low content in Northeastern Dust Region. Additionally, the ratios of Ca/Al at both Northern Dust Region and Northeastern Dust Region were lower than that in Western Dust Region [*Hseung and Jackson*, 1952], for example, 2.04 at Aksu near Taklimakan Desert [*X. Y. Zhang et al.*, 2003] and 3.07 (±1.16) at Taklimakan Desert [*Makra et al.*, 2002], but much higher than the 0.45 of the mean crust abundance [*Mason and Moore*, 1982]. As mentioned above, the high ratio of Ca/Al at BNU, close to those

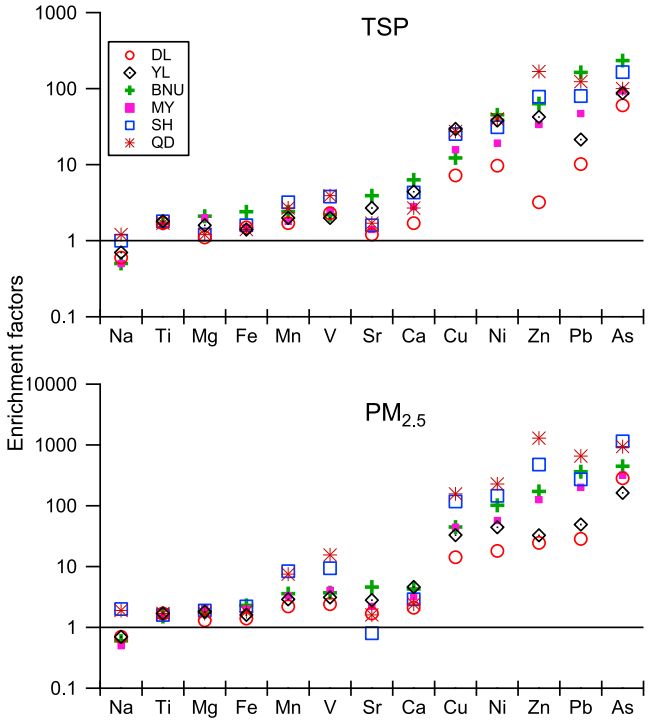

Figure 4. Enrichment factors of the elements in TSP and $PM_{2.5}$ in the spring of 2004.

reported by *He et al.* [2001] could be related to the local construction dust. Overall, the Ca/Al ratio from this study further distinguished the regions and supported the regional division above. The ratio of Ca/Al is thus suggested to be an element tracer to identify the sources of DS in those regions without significant local dust contribution.

3.2.2. Variation of Pollution Elements in Different Regions

[17] Figure 3 presents the spatial variations of pollution elements, As, Zn, Pb, and Cu. An obvious characteristic of the spatial distribution was that the concentrations of pollution elements at DL in region III were distinctively lower than those in other regions. The concentrations of these pollution elements, especially in fine particles in the coastal developed cities, e.g., QD and SH, and inland cities, e.g., BJ, were much higher than those near dust source regions. The sampling sites near source regions are close to the deserts or sandy lands with less anthropogenic sources and more frequent cold fronts, which consequently leads to the lower concentrations of pollution elements. As and Pb at BNU, Zn at QD, and Cu at SH showed the highest concentration among all sites. The high concentrations of these elements at different sites are generally associated with local sources given that they have significant contribution of anthropogenic sources from vehicle emission, industrial emission, and coal combustion during NDS days [*Z. G. Guo et al.*, 2004; *Sun et al.*, 2004b; *Wang et al.*, 2006; *Wei et al.*, 1999].

[18] Enrichment factor (EF, $EF = (X/Al)_{aerosol}/(X/Al)_{crust}$, Al is a reference element) [*Taylor and McLennan*, 1995] is usually used to indicate the contribution of anthropogenic source to a certain element [*Choi et al.*, 2001]. Figure 4 shows that the EFs of Cu, Zn, and Pb at DL in Northeastern Dust Region were ~10, much lower than those in other regions, indicating that these elements were less influenced by anthropogenic sources and Northeastern Dust Region was a relatively clean region [*Sun et al.*, 2005]. DS, if passing through this region, would carry less pollutants and exert more diluting effect on the pollutants in downwind cities [*J. Guo et al.*, 2004]. The high EF of As at DL in TSP (60) and $PM_{2.5}$ (240) was likely from local coal combustion and the high content of As in the soil of northern China [*Wei et al.*, 1999]. YL in Northern Dust Region showed higher EFs of pollution elements than DL, which was likely due to the pollutants transported from the areas surrounding YL [*Hou et al.*, 2006]. The higher EFs of pollution elements at QD and SH in Coastal Region than in other regions were mainly caused by the local pollution sources with less dust contribution. This is supported by the higher EFs during NDS than during DS [*Wang et al.*, 2007]. However, the still high EFs during DS may be partially due to the mixing with pollutants on a longer transport pathway. The pollution elements were more enriched in fine particles, which was suggested by the higher EFs in $PM_{2.5}$ than in TSP. In region IV, which is closer to source regions than Coastal Region, the EFs were lower than those in Coastal Region. Previous studies have shown that some pollution elements, e.g., Zn and Cu, can be from anthropogenic sources and/or long-range transport of dust [*J. Guo et al.*, 2004; *Sun et al.*, 2005]. The lower EFs in region IV indicated that the pollution could be diluted more by DS and has more contribution from mineral sources. Overall, the pollution elements showed significant regionality along Desert Region-Inland Passing Region-Coastal Region, with an increase of their EFs in $PM_{2.5}$ in the order Coastal Region (QD/SH) > Inland Passing Region (BNU/MY) > Northern Dust Region (YL) > Northeastern Dust Region (DL).

3.2.3. Variation of Water-Soluble Ions in Different Regions

[19] Figure 5 presents the spatial variations of Na^+, Mg^{2+}, Ca^{2+}, and K^+. Similar to the mineral elements above, the concentrations of major mineral ions at DL in Northeastern Dust Region were distinctively lower than those in other regions. For example, the concentration of Na^+ decreased in the order QD > YL/SH > BNU > MY > DL. Na^+ correlated well with Al, an indicator of mineral aerosol [*Arimoto et al.*, 2004; *J. Guo et al.*, 2004], in both TSP and $PM_{2.5}$ at YL and BNU ($r = 0.75–0.87$), indicating that Na^+ in the aerosol over YL and BNU was mostly likely from mineral sources. Although correlations between Na^+ and Al were also observed at QD ($r = 0.60$) and SH ($r = 0.77$) in $PM_{2.5}$, the ratio Na^+/Al during NDS (0.39 ± 0.27 for QD and 0.37 ± 0.20 for SH) was much higher than that during DS (0.07 ± 0.03 for QD and 0.18 ± 0.02 for SH), demonstrating the dust impact on Na^+ at QD and SH in region V during DS with large contribution from sea salt to Na^+ during NDS [*Wang et al.*, 2006; *Zhang et al.*, 2001]. Na^+ was weakly correlated with Al ($r = 0.40$ and 0.52 for TSP and $PM_{2.5}$, respectively) at DL as compared to those at YL and BNU, which was likely due to the additional sources for Na^+ from dried salt lake saline soils in arid and semiarid areas [*Zhang et al.*, 2004]. The spatial variations of Mg^{2+} and Ca^{2+}, were in the order YL/BNU > MY > QD/DL, which were similar to the variations of Mg and Ca. The spatial variation of K^+ was much different from other mineral ions. The concentration

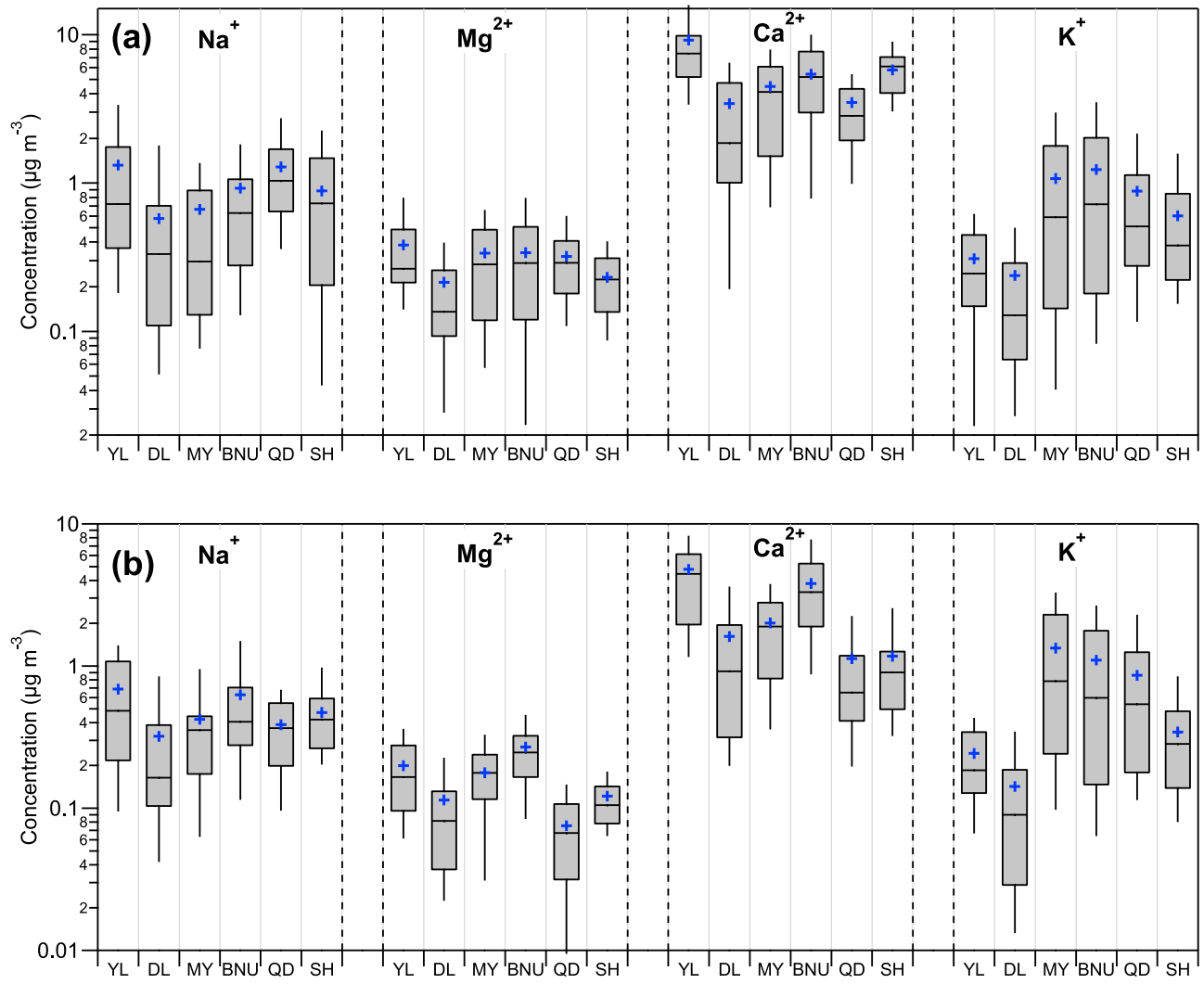

Figure 5. Spatial variations of Na^+,Mg^{2+},Ca^{2+}, and K^+ in (a) TSP and (b) $PM_{2.5}$ in the spring of 2004. Crosses represent the average mass concentration; horizontal lines represent the median; bottom and top of the boxes represent the 25 and 75% limits, respectively; and bottom and top whiskers represent the 5 and 95% limits, respectively.

of K^+ was in the order BNU/MY > QD/SH > YL/DL. The highest concentration of K^+, which is generally used as a marker of biomass burning, at BNU and MY in both TSP and $PM_{2.5}$ was associated with the biomass burning in Beijing and its surrounding areas [*Duan et al.*, 2004].

[20] SO_4^{2-} and NO_3^- in TSP increased in the order YL/DL < MY < BNU < QD < SH (Figure 6a). The spatial distribution of NH_4^+ was similar to that of SO_4^{2-} because NH_4^+ exists mainly in the form of $(NH_4)_2SO_4$ in aerosol particles [*Y. Wang et al.*, 2005b; *Yao et al.*, 2002]. SO_4^{2-} and NO_3^- are mainly from secondary gas-to-particle formation of gases SO_2 and NO_x. The much lower concentrations of SO_4^{2-} and NO_3^- at YL and DL were associated with the low emissions of gaseous SO_2 and NO_x in both region II and region III [*Streets et al.*, 2003; *Zhang et al.*, 2007]. Moreover, the dry air mass near dust source regions with lower relative humidity (RH) at YL and DL (Table 2) was not favorable for the secondary transformation of SO_2 and NO_x, respectively. Comparatively, the large emission of NO_x from motor vehicles and SO_2 from coal combustion plus the high RH both favored the formation of secondary aerosols at QD/SH in Coastal Region. Studies have shown that SO_4^{2-} could also be from crustal sources in addition to the secondary sources near dust source regions [*Sun et al.*, 2005; *Yuan et al.*, 2006]. For example, SO_4^{2-} correlated well with Al at YL (r = 0.70), and the concentration of SO_4^{2-} during DS was synchronously elevated ~2–4 times as Al. Our recent studies found that most of the sulfur in the dust aerosol from Taklimakan Desert, one of the dust sources of YL, was in the form of sulfate [*Huang et al.*, 2010]. The results here supported that SO_4^{2-} can be from both secondary and crustal sources in some dust source regions [*Nishikawa et al.*, 1991]. In comparison to SO_4^{2-}, NO_3^- did not show strong correlations with Al, and furthermore the concentration remained unchanged or even decreased during DS, indicating the different sources of nitrate and sulfate near dust source regions.

[21] The ratio of NO_3^-/SO_4^{2-} is commonly used to indicate the relative contribution of mobile and stationary sources based on that NO_x is mainly from vehicle emission (gasoline

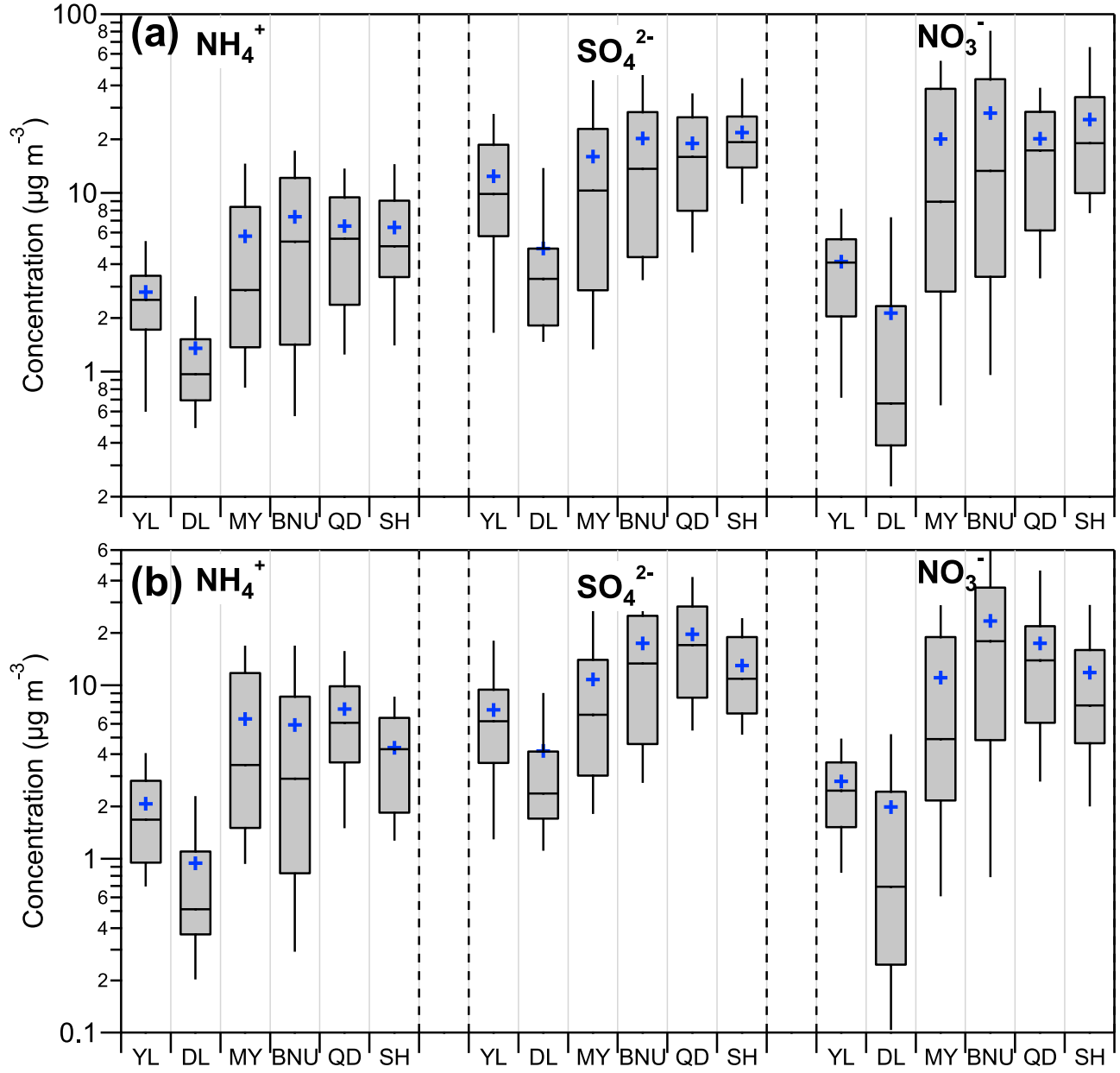

Figure 6. Spatial variations of NH_4^+,NO_3^-,and SO_4^{2-} in (a) TSP and (b) $PM_{2.5}$ in the spring of 2004. Crosses represent the average mass concentration; horizontal lines represent the median; bottom and top of the boxes represent the 25 and 75% limits, respectively; and bottom and top whiskers represent the 5 and 95% limits, respectively.

and diesel combustion) and SO_2 is mainly from coal combustion [*Arimoto et al.*, 1996; *Yao et al.*, 2002]. Figure 7 shows the ratio of NO_3^-/SO_4^{2-} and the concentration of Al at the six sampling sites in spring of 2004. The ratio of NO_3^-/SO_4^{2-} during dust episodes (section 3.3.1) was much lower than those during NDS days, and the lowest value generally appeared after the peak of dust episode. While during NDS days, region II (YL) and region III (DL) showed lower NO_3^-/SO_4^{2-} ratio than those in other regions, which was due to the less mobile sources in these two regions. When the air mass with low NO_3^-/SO_4^{2-} ratio from regions II and III passes through regions IV and V, it would dilute the high ratio of NO_3^-/SO_4^{2-} in these regions, and lead to a lower ratio during dust episodes than during NDS days. Another explanation for the low NO_3^-/SO_4^{2-} ratio is the reactions between HNO_3 in gas phase and carbonates on soil particles (equation (1)) [*Mamane and Gottlieb*, 1992]. This reaction tends to form coarse-mode nitrate that represents a significant sink for NO_x. The lowest NO_3^-/SO_4^{2-} ratio, generally appearing after the peak of dust is likely due to the gradual dry deposition of dust and coarse mode nitrate.

$$2HNO_3(g) + CaCO_3(s) \rightarrow Ca(NO_3)_2(s) + H_2O + CO_2(g). \quad (1)$$

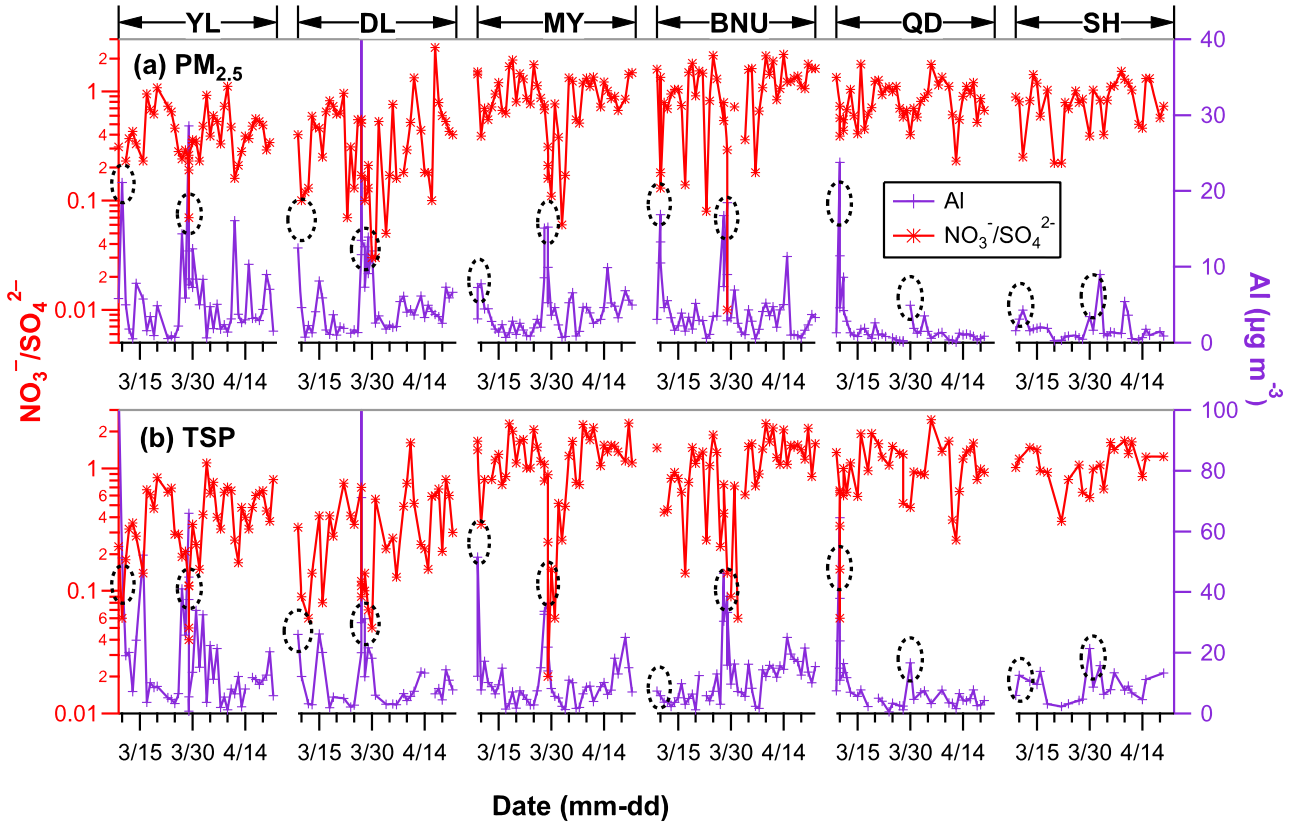

Figure 7. Ratio of NO_3^-/SO_4^{2-} and concentration of Al in (a) TSP and (b) $PM_{2.5}$ at six sites in the spring of 2004. The dust episodes are marked as ovals.

3.3. Impact of Asian Dust on Aerosol Chemistry Over Northern China

3.3.1. Dust Episodes

[22] Two dust events which are marked in Figure 7 occurred over northern China in the spring of 2004. One was from 9–11 March (DS1), and the other was from 27–30 March (DS2). Specifically, 28–29 March at BNU, 9 March and 28–29 March at MY, 9 March and 27–28 March at DL, 9–10 March and 29 March at YL, and 10 March and 30 March at QD and SH were defined as DS days in this study. Most of the areas over northern China experienced the first dust peak on 9 March. The air pollution index (API) in Lanzhou, Xining, Hohhot, and Beijing was up to 500 (>600 $\mu g\ m^{-3}$, named "heavy pollution") on that day (daily report of air quality by State Environmental Protection Administration of China) followed by a significant increase of $PM_{2.5}$ at Qingdao on 10 March. The intensity of DS2 at most sites on 28–30 March was relatively weaker in comparison to DS1, and the concentration of PM_{10} in most of areas over northern China was in the range of 200–400 $\mu g\ m^{-3}$. The back trajectories for DS1 and DS2 at five cities in this study were calculated and shown in Figure 8. Given that the back trajectories staring at different heights were very similar (auxiliary material Figure S1), only those at 1000 m height were used for interpretation. Figure 8 shows that the sources of DS1 and DS2 were different.[1] While DS1 at DL, YL, and BJ originated from the west of China and exerted little effect on SH, DS2 at most of cities except DL originated from Mongolia and the northwest of China.

3.3.2. Impact of Dust on Northern Dust Region and Northeastern Dust Region

[23] The compositional differences between DS and NDS days at DL in Northeastern Dust Region and YL in Northern Dust Region are shown in Figure 9. The concentrations of most mineral elements and mineral ions in both TSP and $PM_{2.5}$ in DS2 at DL were ~5–15 (Fe in TSP even up to 25) of those in NDS days (Figure 9b). The concentrations of

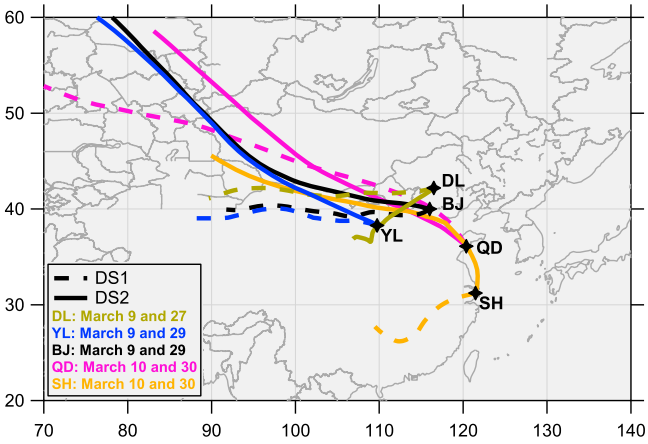

Figure 8. The 48 h back trajectories ending at 0600 UTC at 1000 m above ground level for the two dust events (solid lines, DS1; dashed lines, DS2) in five cities.

[1] Auxiliary materials are available in the HTML. doi:10.1029/2009JD012757.

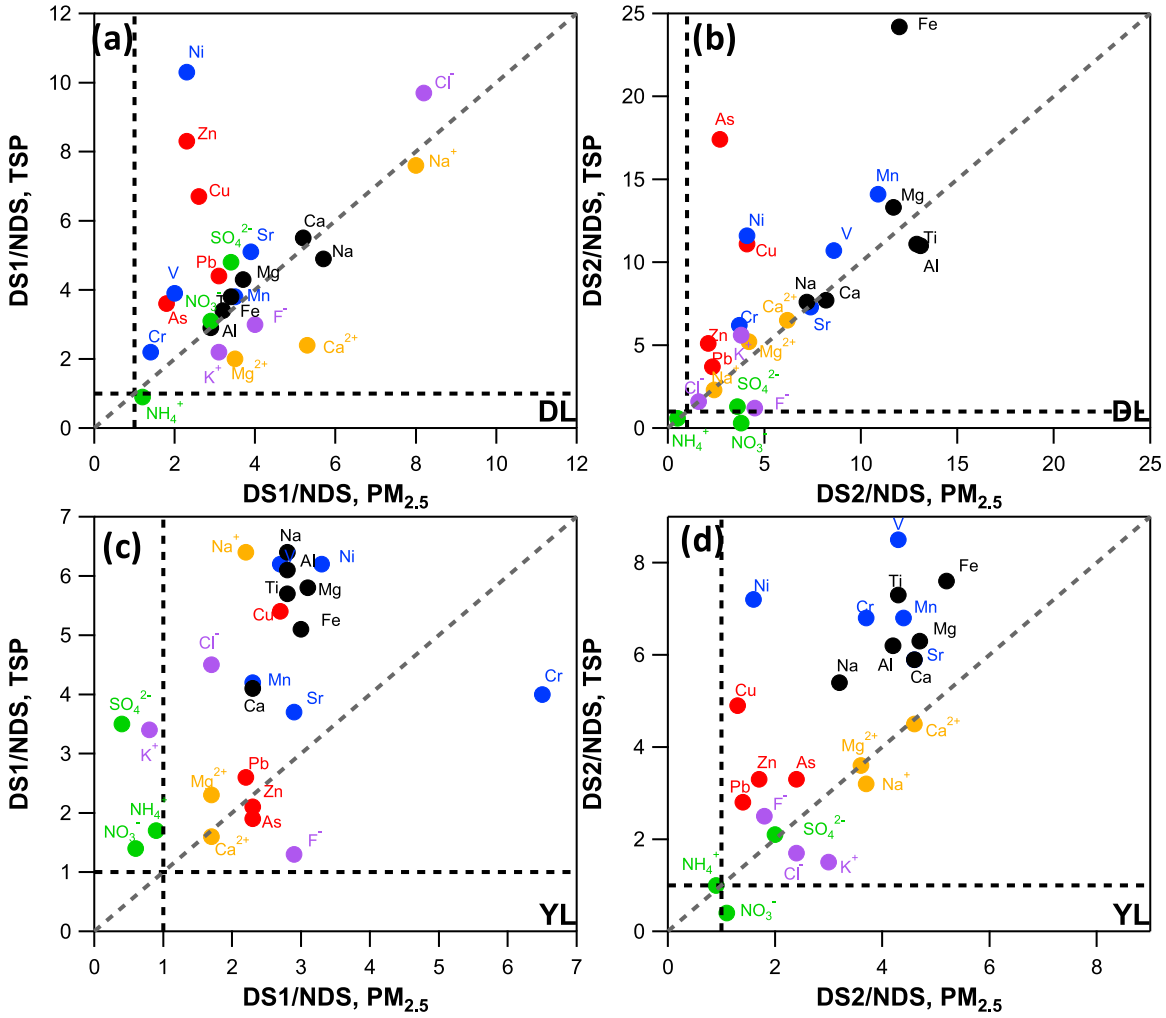

Figure 9. Compositional differences for TSP and $PM_{2.5}$ between dust storm (DS1 and DS2) and nondust storm (NDS) at (a and b) DL and (c and d) YL in the spring of 2004. The vertical and horizontal dashed lines indicate that the ratio of DS to NDS for aerosol components is 1, and the diagonal line represents the 1:1 line.

pollution elements in DS2 were ~5–10 times for TSP and ~2–3 times for $PM_{2.5}$ of those in NDS. These results indicated that DS has strong impact on both mineral and pollution elements near dust source regions, and this impact is more significant on TSP than $PM_{2.5}$. Similar impact of DS on mineral and pollution elements was also observed for DS1 at DL (Figure 9a). The intensity of DS1 was weaker than DS2 and the impact of dust on aerosol chemistry at DL was accordingly weaker. The concentrations of most chemical species in both TSP and $PM_{2.5}$ in DS1 were ~4–6 times of those in NDS, and even higher for pollution elements in TSP. It should be noted that the impact of DS on pollution elements was more significant for TSP than $PM_{2.5}$ in both DS1 and DS2. Given that pollution elements are more enriched in fine particles and mineral elements are more concentrated in coarse particles, results here supported that the pollution elements near dust source regions could have significant mineral contribution. The impact of DS on the water-soluble ions in both DS1 and DS2 was smaller than that on mineral components because water-insoluble mineral components contributed most of dust particles during DS [*Yuan et al.*, 2006]. The significant increase of Na^+, Cl^-, and SO_4^{2-} in DS1 at DL could be related to the dried salt lake saline soils nearby [*Zhang et al.*, 2004]. The impact of DS on mineral elements in TSP at YL was more significant, approximately a factor of 1.5 above the 1:1 line in Figures 9c and 9d, than those in $PM_{2.5}$. While the concentrations of pollution elements were both elevated ~2–3 times in both DS1 and DS2, the impact of DS on them was smaller than mineral elements, which was consistent with those observed at DL. The impact of DS on secondary ions (SO_4^{2-}, NO_3^-, and NH_4^+) was dependent on the relative contribution of anthropogenic and crustal sources, and this impact was sometimes significant between TSP and $PM_{2.5}$. For example, the secondary ions at YL during DS1 were all elevated in TSP in comparison to the decrease in $PM_{2.5}$, suggesting the potential mineral source of secondary ions during DS1 [*Nishikawa et al.*, 1991].

3.3.3. Impact of Dust on Inland Passing Region

[24] Figure 10 presents the comparison of chemical composition between DS and NDS at BNU and MY in region IV. DS1 showed a universally positive impact on all

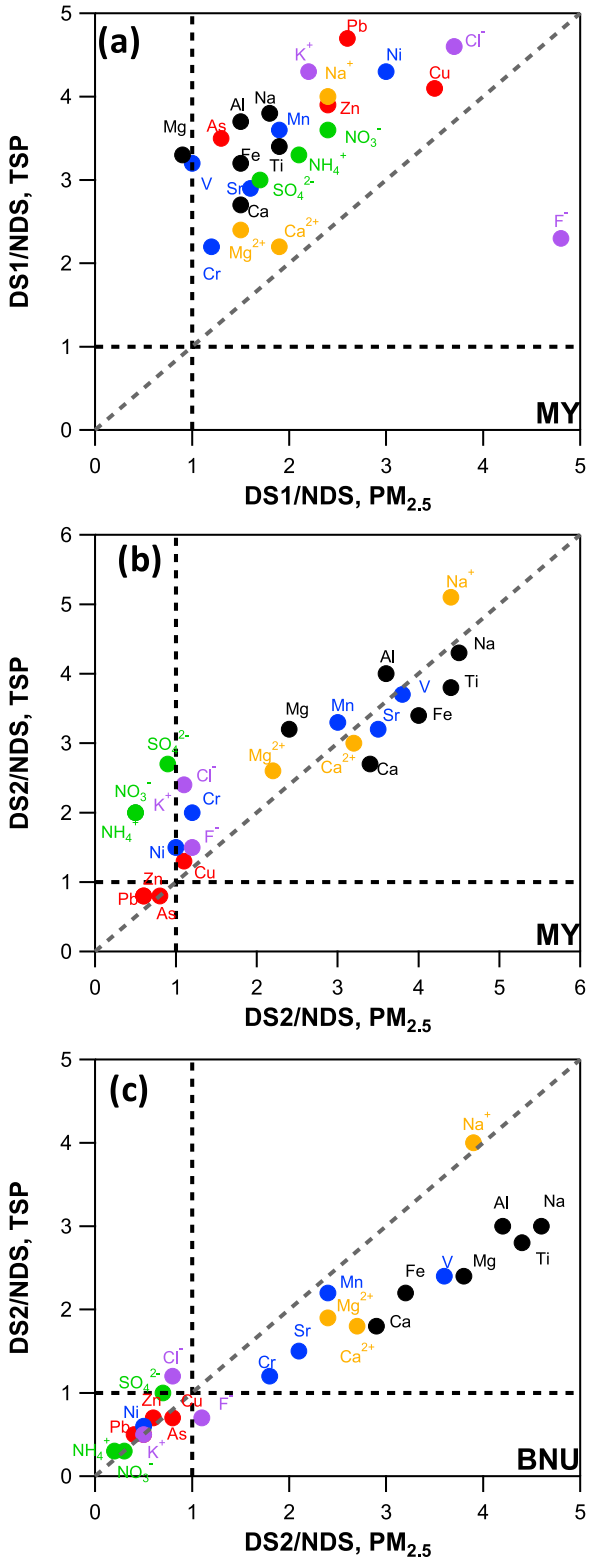

Figure 10. Compositional differences for TSP and $PM_{2.5}$ between dust storm (DS1 and DS2) and nondust storm (NDS) at (a and b) MY and (c) BNU in the spring of 2004. The vertical and horizontal dashed lines indicate that the ratio of DS to NDS for aerosol components is 1, and the diagonal line represents the 1:1 line.

chemical species except F^- in both TSP and $PM_{2.5}$ at MY (Figure 10a), and this impact was more significant on TSP than $PM_{2.5}$, and pollution elements (e.g., Zn, Pb, and Cu) than mineral elements (e.g., Al, Fe, Ca, and Mg). An explanation for this is that DS1 originated from the west (Figure 8) and could bring more pollutants on the pathway. In comparison to DS1, though the mineral elements and ions in both TSP and $PM_{2.5}$ at BNU and MY were elevated by a factor of ~2–5 (Figures 10b and 10c), the pollution elements and secondary ions remained unchanged and even decreased. DS2 originated from region III, which has been proved to be a clean region [*Streets et al.*, 2003; *Sun et al.*, 2005], produced more negative, i.e., diluting, effects on the pollutants in the cities given that it would not carry much pollution on the pathway. It was also observed that the impact of dust on the mineral species in $PM_{2.5}$ was more significant than those in TSP at BNU (Figure 10c). This was likely because of gravitational deposition of coarse particles during the long-range transport of DS, and fine particles could be transported to a longer distance for its longer residence time in the atmosphere. Additionally, the ratios of DS/NDS for mineral species observed in region IV were smaller than those in region II and region III, indicating that the impact of DS weakened gradually as the increase of distance from dust source regions [*Wang et al.*, 2007].

3.3.4. Impact of Dust on Coastal Region

[25] The comparison of aerosol composition between DS and NDS at QD and SH are shown in Figure 11. DS1 showed most impact on mineral elements by a factor of ~4–8 and ~4–12 for TSP and $PM_{2.5}$ respectively at QD. The pollution elements Zn and Pb during DS1 in both TSP and $PM_{2.5}$ remained at the same level, while As and Cu was elevated by a factor of ~2–3. As shown in Figure 11a, the impact of DS1 on the mineral elements in $PM_{2.5}$ was more significant than those in TSP, which further supported that the effect of dust is more significant on fine particles than coarse particles in the areas far from dust source regions. In comparison to DS1, DS2 showed the positive impact on mineral species and negative impact on pollution elements and secondary ions (Figure 11b). A comparison of aerosol composition between DS1 and DS2 revealed that most species in TSP in DS1 were ~1–2 times those in DS2, and even higher in $PM_{2.5}$ (4.4 for Zn, 6.1 for Pb, 4.5 for SO_4^{2-}, and 7.3 for NO_3^-). This was partially due to the different intensities of DS1 and DS2. Although back trajectories in Figure 8 showed the similar transport pathway between DS1 and DS2, DS1 with stronger intensity (section 3.1) could mix more pollution on the pathway than DS2. In addition, the higher RH (42%, Table 2) during DS1 than DS2 (29%) favored the accumulation of pollution. The impact of DS on SH, which is far from the dust source regions, is the smallest among all sites in this study. The mineral species were elevated ~1–3 times during DS2 followed by a decrease of pollution elements (except As) and secondary ions. One of the reasons for the decrease of pollution elements was that the air mass spent ~1 day over the ocean before reaching SH. Back trajectories showed that DS1 did not pass through SH, and SH during DS1 was most affected by the air mass from the southwest of China. Therefore, a synchronous increase for both mineral and pollution elements were observed during DS1, owing to the regional transport from the southwest of China.

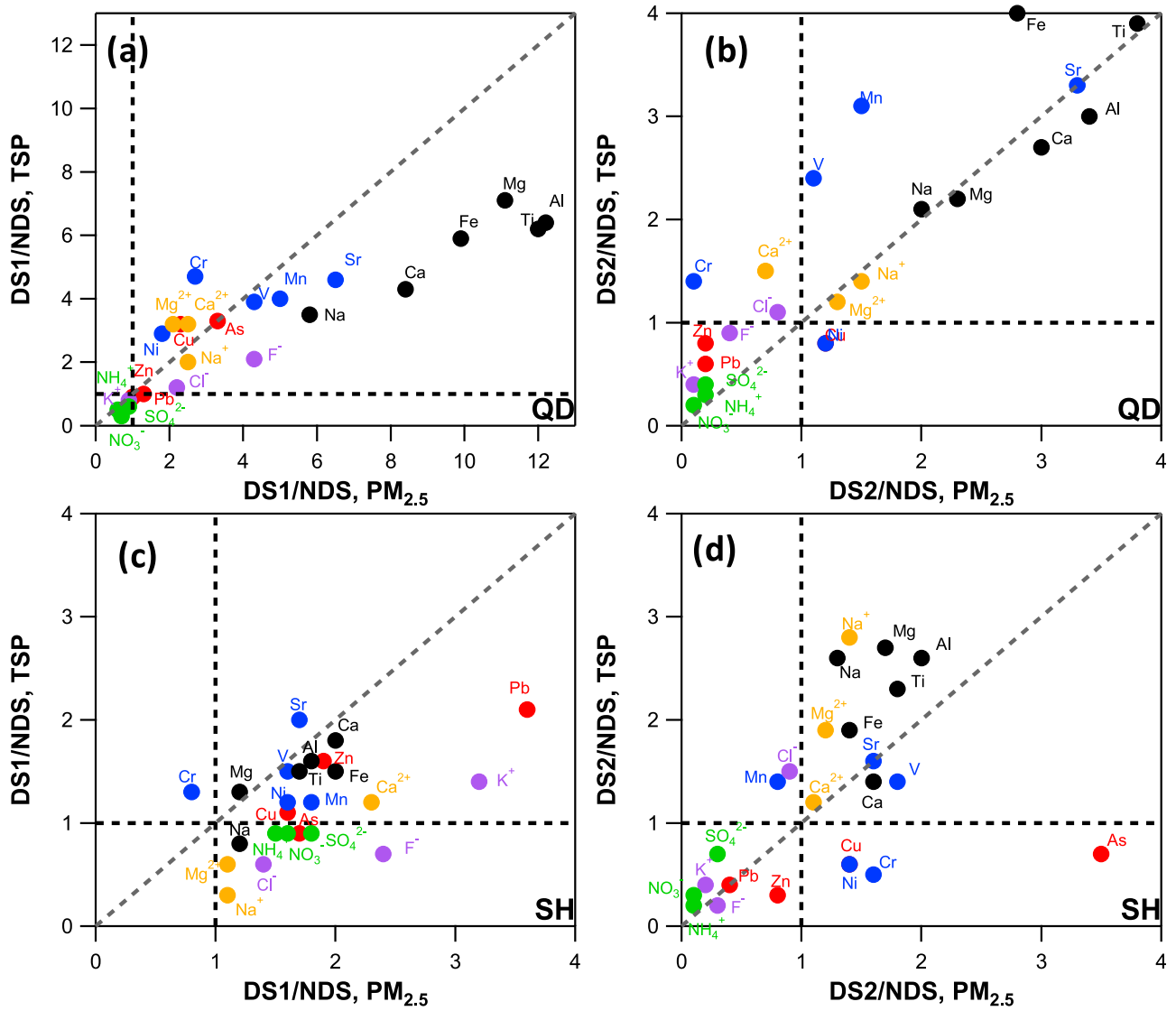

Figure 11. Compositional differences for TSP and $PM_{2.5}$ between dust storm (DS1 and DS2) and nondust storm (NDS) at (a and b) QD and (c and d) SH in the spring of 2004. The vertical and horizontal dashed lines indicate that the ratio of DS to NDS for aerosol components is 1, and the diagonal line represents the 1:1 line.

[26] Overall, investigation the impact of DS on aerosol composition in different regions suggested the following (1) DS showed the most significant impact on the aerosol composition in the regions near dust sources, and the intensity of impact decreased as the increase of distance from source regions, i.e., YL/DL > BNU/MY > QD/SH. (2) The impact of DS on aerosol species in the regions near dust sources was more significant in coarse particles than fine particles, and this impact was reversed in downwind regions far from dust sources. (3) Asian dust produced single positive effect on mineral components, and accumulating or diluting effects on pollutants. DS either mixes the pollutants on the pathway and carries them to downstream regions or dilutes the local pollutants in downwind regions. (4) The sources and transport pathway are two critical factors affecting the aerosol compositions in downwind regions.

3.3.5. Impact of Dust on the Acidity of Aerosol

[27] The equivalent ratio of total cations (Σ+) to total anions (Σ−) of water-extract aerosol particles could be used to indicate the acidity of aerosols [*Y. Wang et al.*, 2005b]. Low pH is mainly due to the acidic components in aerosol particles, such as SO_4^{2-}, NO_3^-, Cl^-, and organic acids, and high pH is generally associated with a high concentration of the basic components, such as NH_4^+, Mg^{2+}, and Ca^{2+}. Our previous studies found that coarse particles showed more alkalinity than fine particles because of the higher concentration of carbonate in coarse particles [*Y. Wang et al.*, 2005b]. Calcium carbonate in dust particles forms sulfate and nitrate via surface reactions with acidic gases, e.g., H_2SO_4 and HNO_3, which was supported by the good correlations between sulfate/nitrate and water-soluble Ca, i.e., Ca^{2+} [*Kim and Park*, 2001; *Nishikawa et al.*, 1991]. This process will be critical to alleviate the acidity of aerosol downstream given the large fraction of calcium carbonate in dust aerosol.

[28] To further investigate the impact of dust on the acidity of aerosol in downwind regions, the correlations of pH and Ca^{2+} were checked and shown in Figure 12. Con-

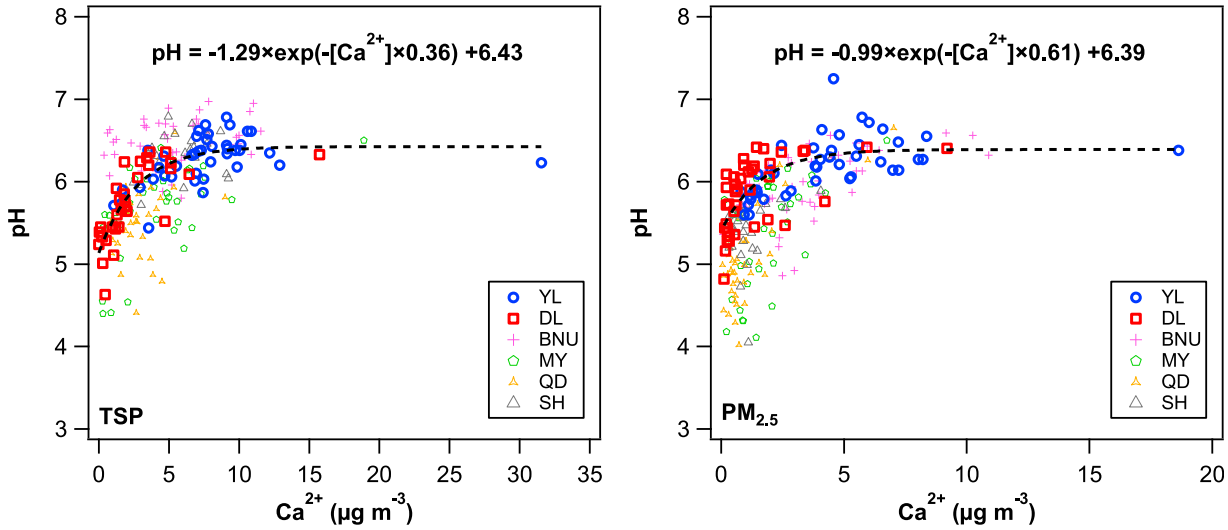

Figure 12. Correlations between pH and water-soluble Ca^{2+} in TSP and $PM_{2.5}$. The fit was performed on the data from YL and DL. Data from other four sites are also shown for reference.

sistent with *Y. Wang et al.* [2005b], the pH was positively associated with the concentration of Ca^{2+}, and showed higher value for TSP than $PM_{2.5}$ in all downwind cities (auxiliary material Figure S2). The average pH for $PM_{2.5}$ at BNU in spring 2004 was 5.95, close to the 5.99 reported in the spring of 2003 [*Y. Wang et al.*, 2005b]. Moreover, the pH in spring is ubiquitously higher than that observed in other seasons, indicating that Asian dust has significant buffering effect on the acidity of aerosol in downwind regions, and this impact is most significant in spring dust season. The positive correlations between pH and Ca^{2+} further confirmed that Ca^{2+} from mineral aerosol could play the most important role in buffering and neutralizing the acidity of aerosol over northern China. YL and DL near dust source regions are less affected by anthropogenic sources and better sites to characterize the impact of Asian dust on the acidity of aerosol. As shown in Figure 12, the pH showed strong exponential correlations with Ca^{2+} in both TSP ($r = 0.85$) and $PM_{2.5}$ ($r = 0.73$) at these two sites. Assuming that the concentration of Ca^{2+} in TSP ranged from 0 to 15 $\mu g\ m^{-3}$, the pH, calculated from the regression equation, varied from 5.1 to 6.4; as such, the pH ranged from 5.4 to 6.4 when the concentration of Ca^{2+} in $PM_{2.5}$ increased from 0 to 9 $\mu g\ m^{-3}$. The pH for TSP and $PM_{2.5}$ both showed a remarkable increase of ~1 unit due to the buffering effect of spring Asian dust. This result was consistent with the simulation results that the annual mean pH values showed a remarkable increase of 0.8–2.5 in northern China and Korea due to the strong neutralization of precipitation by dust aerosols over northeast Asia [*Wang et al.*, 2002].

4. Conclusions

[29] This study systematically investigated the regional characteristics of spring aerosol and the impact of Asian dust on aerosol chemistry over northern China. PM_{10} in the cities of northern China showed significant regionality, based on which northern China could be divided into five regions, i.e., Northern Dust Region, Northeastern Dust Region, Western Dust Region, Inland Passing Region, and Coastal Region. Northern Dust Region and Western Dust Region were characterized by the high content of Ca and the Ca/Al ratio, while Northeastern Dust Region was characterized by low Ca content and Ca/Al ratio. Northeastern Dust Region showed overall the lowest mass loadings and was defined as a clean region. Inland Passing Region and Coastal Region are located in the much more "polluted" regions. Also, most of the cities in Inland Passing Region and Coastal Region showed high concentrations of pollutants.

[30] Asian dust showed the most impact on the aerosol composition in the regions near dust sources, and this impact decreased as the distances from dust sources increased, i.e., Northern Dust Region/Northeastern Dust Region > Inland Passing Region > Coastal Region. The impact of DS on the chemical species of aerosol in the regions near dust sources was more significant in coarse particles than fine particles, and this impact was reversed in downwind regions. Asian dust either mixes the pollutants on the pathway and carries them to downwind regions or dilutes the pollutants over northern China. The ratio of NO_3^-/SO_4^{2-} during DS was significantly reduced, and the lowest generally appeared after the peak of dust. Our study confirmed that Asian dust played an important role in buffering and neutralizing the acidity of aerosol over northern China, which can potentially lead to an increase of ~1 unit of pH in the aerosols in spring.

[31] **Acknowledgments.** We thank the anonymous reviewers for their helpful comments. This work was supported by the National Key Project of Basic Research of China (grant 2006CB403704) and National Natural Science Foundation of China (grants 20877020, 40575062, and 40599420).

References

Arimoto, R., R. A. Duce, D. L. Savoie, J. M. Prospero, R. Talbot, J. D. Cullen, U. Tomza, N. F. Lewis, and B. J. Ray (1996), Relationships among aerosol constituents from Asia and the North Pacific during PEM-West A, *J. Geophys. Res.*, *101*(D1), 2011–2023, doi:10.1029/95JD01071.

Arimoto, R., X. Y. Zhang, B. J. Huebert, C. H. Kang, D. L. Savoie, J. M. Prospero, S. K. Sage, C. A. Schloesslin, H. M. Khaing, and S. N. Oh (2004), Chemical composition of atmospheric aerosols from Zhenbeitai, China, and Gosan, South Korea, during ACE-Asia, *J. Geophys. Res.*, *109*, D19S04, doi:10.1029/2003JD004323.

Cheng, T., D. Lu, G. Wang, and Y. Xu (2005), Chemical characteristics of Asian dust aerosol from Hunshan Dake Sandland in Northern China, *Atmos. Environ.*, *39*(16), 2903–2911, doi:10.1016/j.atmosenv.2004.12.045.

Choi, J. C., M. Lee, Y. Chun, J. Kim, and S. Oh (2001), Chemical composition and source signature of spring aerosol in Seoul, Korea, *J. Geophys. Res.*, *106*(D16), 18,067–18,074, doi:10.1029/2001JD900090.

Dan, M., G. Zhuang, X. Li, H. Tao, and Y. Zhuang (2004), The characteristics of carbonaceous species and their sources in PM2.5 in Beijing, *Atmos. Environ.*, *38*(21), 3443–3452, doi:10.1016/j.atmosenv.2004.02.052.

Duan, F., X. Liu, T. Yu, and H. Cachier (2004), Identification and estimate of biomass burning contribution to the urban aerosol organic carbon concentrations in Beijing, *Atmos. Environ.*, *38*(9), 1275–1282, doi:10.1016/j.atmosenv.2003.11.037.

Duce, R. A., C. K. Unni, B. J. Ray, J. M. Prospero, and J. T. Merrill (1980), Long-range atmospheric transport of soil dust from Asia to the tropical North Pacific: Temporal variability, *Science*, *209*(4464), 1522–1524, doi:10.1126/science.209.4464.1522.

Guo, J., K. A. Rahn, and G. Zhuang (2004), A mechanism for the increase of pollution elements in dust storms in Beijing, *Atmos. Environ.*, *38*(6), 855–862, doi:10.1016/j.atmosenv.2003.10.037.

Guo, Z. G., J. L. Feng, M. Fang, H. Y. Chen, and K. H. Lau (2004), The elemental and organic characteristics of PM2.5 in Asian dust episodes in Qingdao, China, 2002, *Atmos. Environ.*, *38*(6), 909–919, doi:10.1016/j.atmosenv.2003.10.034.

Han, L., G. Zhuang, S. Cheng, Y. Wang, and J. Li (2007), Characteristics of re-suspended road dust and its impact on the atmospheric environment in Beijing, *Atmos. Environ.*, *41*(35), 7485–7499, doi:10.1016/j.atmosenv.2007.05.044.

He, K., F. Yang, Y. Ma, Q. Zhang, X. Yao, C. K. Chan, S. Cadle, T. Chan, and P. Mulawa (2001), The characteristics of PM2.5 in Beijing, China, *Atmos. Environ.*, *35*(29), 4959-4970, doi:10.1016/S1352-2310(01)00301-6.

Hou, X., G. Zhuang, Y. Sun, and Z. An (2006), Characteristics and sources of polycyclic aromatic hydrocarbons and fatty acids in PM2.5 aerosols in dust season in China, *Atmos. Environ.*, *40*(18), 3251–3262, doi:10.1016/j.atmosenv.2006.02.003.

Hseung, Y., and M. L. Jackson (1952), Mineral composition of the clay fraction: III. Of some main soil groups of China, *Soil Sci. Soc. Am. J.*, *16*(3), 294.

Huang, K., G. Zhuang, J. Li, Q. Wang, Y. Sun, and J. Fu (2010), The mixing of Asian dust with pollution aerosol and the transformation of aerosol components during the dust storm over China in spring, 2007, *J. Geophys. Res.*, doi:10.1029/2009JD013145, in press.

Huebert, B. J., T. Bates, P. B. Russell, G. Shi, Y. J. Kim, K. Kawamura, G. Carmichael, and T. Nakajima (2003), An overview of ACE-Asia: Strategies for quantifying the relationships between Asian aerosols and their climatic impacts, *J. Geophys. Res.*, *108*(D23), 8633, doi:10.1029/2003JD003550.

Husar, R. B., et al. (2001), Asian dust events of April 1998, *J. Geophys. Res.*, *106*(D16), 18,317–18,330, doi:10.1029/2000JD900788.

In, H.-J., and S.-U. Park (2002), A simulation of long-range transport of Yellow Sand observed in April 1998 in Korea, *Atmos. Environ.*, *36*(26), 4173–4187, doi:10.1016/S1352-2310(02)00361-8.

Jickells, T. D., et al. (2005), Global iron connections between desert dust, ocean biogeochemistry, and climate, *Science*, *308*(5718), 67–71, doi:10.1126/science.1105959.

Kim, B.-G., and S.-U. Park (2001), Transport and evolution of a winter-time Yellow sand observed in Korea, *Atmos. Environ.*, *35*(18), 3191–3201, doi:10.1016/S1352-2310(00)00469-6.

Liu, C. L., J. Zhang, and Z. B. Shen (2002), Spatial and temporal variability of trace metals in aerosol from the desert region of China and the Yellow Sea, *J. Geophys. Res.*, *107*(D14), 4215, doi:10.1029/2001JD000635.

Makra, L., I. Borbély Kiss, E. Koltay, and Y. Chen (2002), Enrichment of desert soil elements in Takla Makan dust aerosol, *Nucl. Instrum. Methods Phys. Res., Sect. B*, *189*(1–4), 214–220, doi:10.1016/S0168-583X(01)01045-X.

Mamane, Y., and J. Gottlieb (1992), Nitrate formation on sea-salt and mineral particles—A single particle approach, *Atmos. Environ.*, *26*(9), 1763–1769.

Mason, B., and C. B. Moore (1982), *Principle of Geochemistry*, 176 pp., John Wiley, Hoboken, N. J.

Meskhidze, N., W. L. Chameides, A. Nenes, and G. Chen (2003), Iron mobilization in mineral dust: Can anthropogenic SO_2 emissions affect ocean productivity?, *Geophys. Res. Lett.*, *30*(21), 2085, doi:10.1029/2003GL018035.

Nishikawa, M., S. Kanamori, N. Kanamori, and T. Mizoguchi (1991), Kosa aerosol as eolian carrier of anthropogenic material, *Sci. Total Environ.*, *107*, 13–27, doi:10.1016/0048-9697(91)90247-C.

Qian, W., X. Tang, and L. Quan (2004), Regional characteristics of dust storms in China, *Atmos. Environ.*, *38*(29), 4895–4907, doi:10.1016/j.atmosenv.2004.05.038.

Song, Y., Y. Zhang, S. Xie, L. Zeng, M. Zheng, L. G. Salmon, M. Shao, and S. Slanina (2006), Source apportionment of PM2.5 in Beijing by positive matrix factorization, *Atmos. Environ.*, *40*(8), 1526–1537, doi:10.1016/j.atmosenv.2005.10.039.

Streets, D. G., et al. (2003), An inventory of gaseous and primary aerosol emissions in Asia in the year 2000, *J. Geophys. Res.*, *108*(D21), 8809, doi:10.1029/2002JD003093.

Sun, Y., G. Zhuang, Y. Wang, L. Han, J. Guo, M. Dan, W. Zhang, Z. Wang, and Z. Hao (2004a), The air-borne particulate pollution in Beijing—Concentration, composition, distribution and sources, *Atmos. Environ.*, *38*(35), 5991–6004, doi:10.1016/j.atmosenv.2004.07.009.

Sun, Y., G. Zhuang, H. Yuan, X. Zhang, and J. Guo (2004b), Characteristics and sources of 2002 super dust storm in Beijing, *Chin. Sci. Bull.*, *49*(7), 698–705.

Sun, Y., G. Zhuang, Y. Wang, X. Zhao, J. Li, Z. Wang, and Z. An (2005), Chemical composition of dust storms in Beijing and implications for the mixing of mineral aerosol with pollution aerosol on the pathway, *J. Geophys. Res.*, *110*, D24209, doi:10.1029/2005JD006054.

Sun, Y., G. Zhuang, W. Zhang, Y. Wang, and Y. Zhuang (2006), Characteristics and sources of lead pollution after phasing out leaded gasoline in Beijing, *Atmos. Environ.*, *40*(16), 2973–2985, doi:10.1016/j.atmosenv.2005.12.032.

Taylor, S. R., and S. M. McLennan (1995), The geochemical evolution of the continental crust, *Rev. Geophys.*, *33*(2), 241–265, doi:10.1029/95RG00262.

Uematsu, M., A. Yoshikawa, H. Muraki, K. Arao, and I. Uno (2002), Transport of mineral and anthropogenic aerosols during a Kosa event over East Asia, *J. Geophys. Res.*, *107*(D7), 4059, doi:10.1029/2001JD000333.

Wang, S., J. Wang, Z. Zhou, and K. Shang (2005), Regional characteristics of three kinds of dust storm events in China, *Atmos. Environ.*, *39*(3), 509–520, doi:10.1016/j.atmosenv.2004.09.033.

Wang, Y., G. Zhuang, Y. Sun, and Z. An (2005a), Water-soluble part of the aerosol in the dust storm season-Evidence of the mixing between mineral and pollution aerosols, *Atmos. Environ.*, *39*(37), 7020–7029, doi:10.1016/j.atmosenv.2005.08.005.

Wang, Y., G. Zhuang, A. Tang, H. Yuan, Y. Sun, S. Chen, and A. Zheng (2005b), The ion chemistry and the source of PM2.5 aerosol in Beijing, *Atmos. Environ.*, *39*(21), 3771–3784, doi:10.1016/j.atmosenv.2005.03.013.

Wang, Y., G. Zhuang, X. Zhang, K. Huang, C. Xu, A. Tang, J. Chen, and Z. An (2006), The ion chemistry, seasonal cycle, and sources of PM2.5 and TSP aerosol in Shanghai, *Atmos. Environ.*, *40*(16), 2935–2952, doi:10.1016/j.atmosenv.2005.12.051.

Wang, Y., G. Zhuang, A. Tang, W. Zhang, Y. Sun, Z. Wang, and Z. An (2007), The evolution of chemical components of aerosols at five monitoring sites of China during dust storms, *Atmos. Environ.*, *41*(5), 1091–1106, doi:10.1016/j.atmosenv.2006.09.015.

Wang, Z., H. Akimoto, and I. Uno (2002), Neutralization of soil aerosol and its impact on the distribution of acid rain over east Asia: Observations and model results, *J. Geophys. Res.*, *107*(D19), 4389, doi:10.1029/2001JD001040.

Wei, F., E. Teng, G. Wu, W. Hu, W. E. Wilson, R. S. Chapman, J. C. Pau, and J. Zhang (1999), Ambient concentrations and elemental compositions of PM10 and PM2.5 in four Chinese cities, *Environ. Sci. Technol.*, *33*(23), 4188–4193, doi:10.1021/es9904944.

Yao, X., C. K. Chan, M. Fang, S. Cadle, T. Chan, P. Mulawa, K. He, and B. Ye (2002), The water-soluble ionic composition of PM2.5 in Shanghai and Beijing, China, *Atmos. Environ.*, *36*(26), 4223–4234, doi:10.1016/S1352-2310(02)00342-4.

Ye, B., X. Ji, H. Yang, X. Yao, C. K. Chan, S. H. Cadle, T. Chan, and P. A. Mulawa (2003), Concentration and chemical composition of PM2.5 in Shanghai for a 1-year period, *Atmos. Environ.*, *37*(4), 499–510, doi:10.1016/S1352-2310(02)00918-4.

Yuan, H., Y. Wang, and G. S. Zhuang (2003), The simultaneous determination of organic acid, MSA with inorganic anions in aerosol and rain-water by ion chromatography, *J. Inst. Anal.*, *6*, 12–16.

Yuan, H., G. Zhuang, K. A. Rahn, X. Zhang, and Y. Li (2006), Composition and mixing of individual particles in dust and nondust conditions of north China, spring 2002, *J. Geophys. Res.*, *111*, D20208, doi:10.1029/2005JD006478.

Zhang, D., J. Zang, G. Shi, Y. Iwasaka, A. Matsuki, and D. Trochkine (2003), Mixture state of individual Asian dust particles at a coastal site of Qingdao, China, *Atmos. Environ.*, *37*(28), 3895–3901, doi:10.1016/S1352-2310(03)00506-5.

Zhang, J., Y. Wu, C. L. Liu, Z. B. Shen, Z. G. Yu, and Y. Zhang (2001), Aerosol characters from the desert region of northwest China and the Yellow Sea in spring and summer: Observations at Minqin, Qingdao, and Qianliyan in 1995–1996, *Atmos. Environ.*, *35*(29), 5007–5018, doi:10.1016/S1352-2310(01)00269-2.

Zhang, Q., et al. (2007), NO_x emission trends for China, 1995–2004: The view from the ground and the view from space, *J. Geophys. Res.*, *112*, D22306, doi:10.1029/2007JD008684.

Zhang, X. Y., G. Zhang, G. Zhu, D. E. Zhang, Z. S. An, T. Chen, and X. P. Huang (1996), Elemental tracers for Chinese source dust, *Sci. China, Ser. D*, *39*, 512–521.

Zhang, X. Y., S. L. Gong, Z. X. Shen, F. M. Mei, X. X. Xi, L. C. Liu, Z. J. Zhou, D. Wang, Y. Q. Wang, and Y. Cheng (2003), Characterization of soil dust aerosol in China and its transport and distribution during 2001 ACE-Asia: 1. Network observations, *J. Geophys. Res.*, *108*(D9), 4261, doi:10.1029/2002JD002632.

Zhang, X. Y., G. S. Zhuang, and H. Yuan (2004), The dried salt-lakes saline soils sources of the dust storm in Beijing-the individual particles analysis and XPS surface structure analysis, *China Environ. Sci.*, *24*(5), 533–537.

Zheng, C., H. M. Li, M. P. Chem, and W. X. Wang (1994), *Atlas of Soil Environmental Background Value in the People's Republic of China*, China Environ. Sci. Press, Beijing.

Zhuang, G. S., Z. Yi, and R. A. Duce (1992), Link between iron and sulfur cycles suggested by detection of iron (II) in remote marine aerosols, *Nature*, *355*(6360), 537–539, doi:10.1038/355537a0.

Zhuang, G., J. Guo, H. Yuan, and C. Zhao (2001), The compositions, sources, and size distribution of the dust storm from China in spring of 2000 and its impact on the global environment, *Chin. Sci. Bull.*, *46*(11), 895–900, doi:10.1007/BF02900460.

J. S. Fu, Department of Civil and Environmental Engineering, University of Tennessee, Knoxville, TN 37996, USA.

K. Huang, J. Li, Y. Lin, Q. Wang, Y. Wang, and G. Zhuang, Center for Atmospheric Chemistry Study, Department of Environmental Science and Engineering, Fudan University, Shanghai 200433, China. (gzhuang@fudan.edu.cn)

Y. Sun, Department of Environmental Toxicology, University of California, Davis, CA 95616, USA.

A. Tang, W. Zhang, and X. Zhao, Center for Atmospheric Environmental Study, Department of Chemistry, Beijing Normal University, Beijing 100875, China.